Chapter 20

Pulsed Power Diagnostics

––*Romesh Chandra, Dr. Rakhee Menon*

Pulsed voltages and currents of hundreds of kilovolts and kilo amperes respectively call for measuring instruments that should offer insignificant impedance so as not to load the system or distort the waveform. They should be calibrated using standard methods as well. Some of the most commonly used voltage and current diagnostics are described below.

20.1. Pulsed high current measurement

Measurement of current waveforms has an additional requirement of having sufficient bandwidth in the measuring probes to reciprocate the pulse nature of the electrical voltage and current pulses.

20.1.1. Rogowski Coil

The transient high current of the order of kA to MA can be measured using Rogowski coils. The advantages are that they are non intrusive, frequency independent output voltage, ease of installation and operation etc. Rogowski coils are wound on toroidal core form, usually with a plastic core and are calibrated using standard cable pulser method. The toroidal core encircles the current to be measured and generates an EMF proportional to the rate of change of current. The voltage induced because of the current threading the coil is given by

$$\frac{d\phi}{dt} = L\frac{dI_c}{dt} + I_c R_c \tag{20.1}$$

where R_c is the current viewing resistor, L is the inductance of the coil, I_c is the current threading the coil. Rogowski coil can be operated in differentiating ($L/R \times dI_c/dt << I_c$) or self integrating ($L/R \times dI_c/dt >> I_c$) forms. For self integrating coils, L/R is typically taken as 10 times the pulse width of the current to be measured. Rogowski coil is placed inside a metal enclosure to prevent stray field interference. The flux linking the coil is given by

$$\phi = \frac{\mu INa^2}{2r} \tag{20.2}$$

Here μ, N, a and r are the permeability, total number of turns, minor turn radius and major radius of the coil respectively.

20.1.2. B-dot Probe

A B-dot probe also relies on measuring the voltage induced in the coil due to inductive coupling. Here the coil does not form a closed loop. The induced voltage for a B-dot loop is given by

$$V_{ind} = \frac{\mu_0 NA}{2\pi r}\frac{dI}{dt} \tag{20.3}$$

Here μ_0, N, A and r are the permeability of free space, number of turns, loop area and distance between current carrying conductor and the B-dot loop respectively. B-dot probe has certain short comings like sensitivity to external flux linkage. They require in situ calibration as they are position dependant. Advantages are that they are easy to make and install.

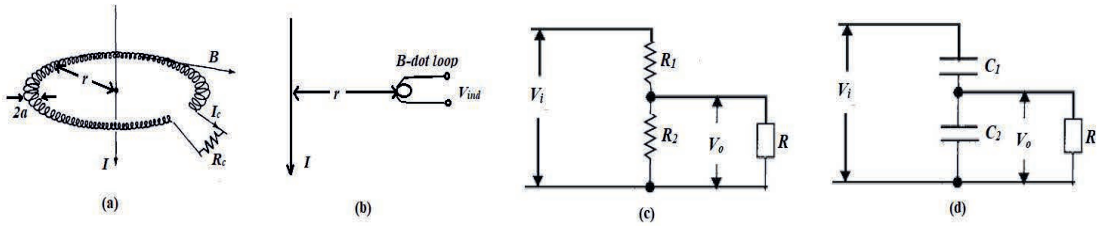

Figure 20.1. Schematic of (a) Rogowski Coil (b) B-dot probe (c) Resistive voltage divider & (d) Capacitive divider. R_c is the current viewing resistor, R is the oscilloscope impedance.

20.2. Pulsed high voltage measurement

Pulse power systems are capable of supplying voltage pulses ranging from 100 kV to 3 MV within 30 ns to 300 ns. Thus the voltage diagnostics must have bandwidth and breakdown strength to measure such high voltages.

20.2.1. Resistive Divider

Aqueous resistive voltage dividers are most commonly used resistive voltage dividers in measuring the high voltage pulse. They have advantages like low inductance, can withstand large electric fields and recovery time is less in case of breakdown. Aqueous copper sulphate ($CuSO_4.5H_2O$) voltage dividers (with copper electrodes) are widely used for measuring the high voltage pulse. The voltage division occurs between tubes of aqueous copper sulphate solution which forms the high voltage arm and a lower arm of usually 1-5 Ω made of parallel carbon resistors. Also, aqueous solutions of NaCl and KCl are also used in measuring the pulsed high voltage. For an input voltage of V_i, the output voltage across low arm resistor, R_2 will be

$$V_o = \left(\frac{R_2}{R_1 + R_2} \right) V_i \tag{20.4}$$

The voltage across resistor is measured at oscilloscopes having sufficient bandwidth at 50 ohm termination at the oscilloscope.

20.2.2. Capacitive Divider

In capacitive voltage divider, two capacitors are connected in series. U_i is the high voltage of the measured electrode, C_1 & C_2 are the high voltage and low voltage arms. R is the impedance of the oscilloscope for measuring voltage.

$$\frac{dV_i}{dt} = \left(\frac{C_1 + C_2}{C_1} \right) \frac{dV_o}{dt}_i + \frac{V_o}{C_1 R} \tag{20.5}$$

when $R(C1 + C2) <<$ pulse width to be measured, an integrator circuit is required, whereas if $R(C1 + C2) >>$ pulse width, the capacitive divider is self integrating.

20.3. Flash X-ray (FXR) Diagnostics

Flash X-rays have very high dose lasting for few nanoseconds. Thus dose rate becomes very high for FXR sources. The diagnostic of FXR includes measurement of accumulated dose, spot size measurement for characterization of FXR source, pulse width measurement and spectrum measurement. For imaging purpose image plates are being used. These are discussed in this section given below,

20.3.1. Dose Measurement

Dose rate is very high for FXR sources. Thermo luminescent dosimeters (TLD) are most commonly used for measuring the dose. The incident radiation energy is stored in the wide band gap of TLD material and on heating, stored energy comes out in visible light form. For increasing the light yield, dopants are added in the TLD base materials. Some of the common TLDs are calcium sulphate doped with dysprosium ($CaSO_4$:Dy), lithium fluoride (LiF), barium sulphate doped with europium ($BaSO_4$:Eu) etc. Direct Reading Dosimeters (DRD) work on the principle of ionisation chamber and usually indicate dose levels of 0–200 mR or 0–500 mR. These are calibrated with standard sources and are commercially available. They are dose rate independent like TLDs.

20.3.2. Spot Size Measurement

Pinhole, roll bar and slit methods can be used in measuring the FXR spot size. A pin hole provides the spot intensity profile and the source size can be the FWHM of the intensity profile of the pinhole image. Time varying FXR spot size can be measured using scintillator arrays coupled to multi channel plate – Photo multiplier tube (MCP-PMT) detectors and pinhole arrays paired with MCP detector set ups.

20.3.3. Pulse Width Measurement

FXR pulse width measurement is usually determined by plastic scintillator based detectors coupled to photo multiplier tubes (PMT). Silicon *p-i-n* diodes can also be used for measuring the x-ray pulse width. Time resolved pulse width can be measured using scintillator arrays or photo diode arrays coupled to multi channel analyzer.

20.3.4. Spectrum Measurement

The attenuation or differential absorption technique is generally used for estimating the energy spectrum from a pulsed hard X-ray source. Here, the dose is recorded by detectors kept behind dissimilar metal filters and the spectrum is unfolded from the measured dose and detector response data. This method is efficient up to 800-900 keV beyond which the detector response is not different enough.

$$Q_i = \sum_j R_i(E_j) S(E_j) \Delta(E_j) \tag{20.6}$$

where i is the filter number and j is the number of energy bins chosen with $j >> i$.

20.3.5. Imaging

For imaging, most sensitive are X-ray films. Computed radiography systems with photostimulable image plates can also be used for image acquisition. When X-ray photons fall on the image plate, the phosphor layer in it stores the image. While scanning, the laser in the image scanner releases the stored image information in visible form and is captured by a photomultiplier tube for converting to electrical signal and stored digitally.

20.4. Microwave Diagnostics

Diagnostics for high power high frequency microwaves require components which are suitable for high frequency capture and transmission. In HPM one has to make sure that the electric field stresses in the entire diagnostic circuit are under electrical breakdown limit.

Far Field Measurements: Far field region is the boundary beyond which antenna pattern is not a function of R, where R is the distance from antenna. Antenna gain is defined for the far field region hence all the measurements are done in the far field region, which expression is given by,

$$R \geq {}^{2D^2}/_{\lambda} \tag{20.7}$$

D is the largest dimension of window and λ is the wavelength of high power microwave radiation. Far field probes must be kept at larger distance from R. Three probes which are used for measurement are given below.

20.4.1. Antenna Measurements

In the antenna measurement setup, measuring antenna is kept in the far field region to receive radiated microwave power. If P_t is the power transmitted by radiating antenna, G_t is the gain of radiating antenna and G_r is the gain of receiving antenna, the power received at receiving antenna is given by [7],

$$P_r(\theta,\phi) = P_t \times G_t(\theta,\phi) \times G_r(\theta,\phi) \times \left(\frac{\lambda}{4\pi R}\right)^2 \tag{20.8}$$

Here λ is the wavelength of the microwave radiation. This formula is valid for far field region only. Another method is to use antenna factor (A.F.). Antenna factor of receiving antenna is defined as the ratio of electric field at the aperture of antenna to the voltage induced at the output of antenna at a matched load (50 ohm in general). In this method, if V_{osc} is the voltage at the matched load then electric field at the receiving antenna is given by,

$$E = V_{osc} \times A.F. \tag{20.9}$$

Peak power density at the receiving antenna position is given by [8],

$$P_d = {}^{E^2}/_{Z_0} \tag{20.10}$$

In this case power transmitted by the source antenna is given by [9],

$$P_t = \frac{P_d \times 4\pi R^2}{G_t} \tag{20.11}$$

Receiving antenna measurements are excellent tool for power measurement. Due to its high sensitivity and low susceptibility towards unwanted reflected fields, it is widely used for far field measurements. It's advantage of high sensitivity is a drawback while measuring very high fields, because it may suffer an electrical breakdown due to its high gain [9].

20.4.2. B-dot probe measurement

B-dot probes consist of a loop which couples with magnetic field lines passing through it. For power measurements it is kept in the far field region in an orientation such that H-field lines pass though the loop area.

If V_{osc} is the voltage recorded in the oscilloscope and B is the magnetic field in the loop, then [10]

$$V_{osc} = A_{eq} \frac{\partial B}{\partial t} \tag{20.12}$$

For narrowband microwave measurements in the far field $\frac{\partial B}{\partial t} = \omega B$ and $E = cB$. From this electrical field value microwave power can be measured.

20.4.3. D-dot probe measurement

D-dot probes capacitively couple to the electric field to generate voltage across its two terminals, when they are kept into it. This measured voltage is V_{osc} then the D-field cab be estimated using the formula given below [11],

$$V_{osc} = RA_{eq} \frac{\partial D}{\partial t} \tag{20.13}$$

For narrowband microwave measurements in the far field $\frac{\partial D}{\partial t} = \omega \varepsilon_0 E$. From this electrical field value microwave power can be measured. Once we know the *E*-field, we can calculate the power transmitted using Eqs. (20.10) and (20.11). This probe is suitable for very high frequency measurements, but suffers from reflections if present.

References

[1] Nassisi, Vincenzo & Luches, Armando. (1979). Rogowski coils: theory and experimental results. Review of Scientific Instruments. 50. 900 - 902. 10.1063/1.1135946.

[2] D. G. Pellinen, M. S. Di Capua, S. E. Sampayan, H. Gerbracht, and M. Wang, "Rogowski coils for measuring fast, high-level pulsed currents," *Rev. Sci. Instrum.* Vol. **51**, pp.1535-1540, 1980.

[3] Jane Lehr and Prahlad Ron, "Foundations of Pulsed Power Technology", ISBN: 9781118886502, Wiley *IEEE* Press, 2017, DOI:10.1002/9781118886502.

[4] Jin-Liang Liu, Bing Ye, Tian-Wen Zhan, Jia-Huai Feng, Jian-De Zhang, and Xin-Xin Wang, "Coaxial Capacitive Dividers for High-Voltage Pulse Measurements in Intense

Electron Beam Accelerator With Water Pulse-Forming Line", *IEEE Transactions on Instrumentation and measurement*, Vol. **58**, No. 1, January 2009.

[5] M.M Brady and K.G Dedrick, "High Voltage Pulse Measurement with a Precision Capacitive Voltage Divider", *Rev. Sci. Instrum.* Vol. **33**, No. 12, pp.1421-1428, 1962.

[6] Rakhee Menon K, A.S Patel, Senthil K, Ankan Basak, R.Kumar, Romesh Chandra, Bhushan Dhabekar, A.K Singh, S.Mitra, Amitava Roy, K.D Joshi and Archana Sharma, "Characterization of Flash X-ray Source from a Marx based Pulse Power System," *IEEE Trans. Plasma Sci.*, vol. **49**, no. 8, pp. 2359 - 2363, August 2021, doi: 10.1109/TPS.2021.3092055.

[7] Harald T. Friis, "A Note on a Simple Transmission Formula," Proceedings of the I.R.E. and Waves and Electrons, May, 1946, pp 254–256.

[8] D.M. Pozar, "Microwave Engineering." 2nd Ed., Wiley, 1998.

[9] Jacobs, Bennie, Johann W. Odendaal, and Johan Joubert. "An improved design for a 1–18 GHz double-ridged guide horn antenna." IEEE Transactions on Antennas and Propagation 60, no. 9 (2012): 4110-4120.

[10] https://www.prodyntech.com/home-page/products/b-dots-magnetic-field-sensors/

[11] https://www.prodyntech.com/home-page/products/d-dots-electric-field-sensors/